The University of Nottingham

UNITED KINGDOM · CHINA · MALAYSIA

Liao, Zhiyu and Sinjab, Faris and Nommeots-Nomm, Amy and Jones, Julian and Ruiz-Cantu, Laura and Yang, Jing and Rose, Felicity R.A.J. and Notingher, Ioan (2017) Feasibility of spatially-offset Raman spectroscopy for in-vitro and in-vivo monitoring mineralisation of bone tissue-engineering scaffolds. Analytical Chemistry, 89 (1). pp. 847-853. ISSN 1520-6882

Access from the University of Nottingham repository:
http://eprints.nottingham.ac.uk/39605/1/Liao%20et%20al%202016%20SORS_reviewed.pdf

A note on versions:

The version presented here may differ from the published version or from the version of record. If you wish to cite this item you are advised to consult the publisher's version. Please see the repository url above for details on accessing the published version and note that access may require a subscription.

For more information, please contact eprints@nottingham.ac.uk

Feasibility of spatially-offset Raman spectroscopy for *in-vitro* and *in-vivo* monitoring mineralisation of bone tissue-engineering scaffolds

Zhiyu Liao,[1] Faris Sinjab,[1] Amy Nommeots-Nomm,[2] Julian Jones,[2] Laura Ruiz-Cantu,[3] Jing Yang,[3] Felicity Rose,[3] and Ioan Notingher[1]*

[1]School of Physics and Astronomy, University of Nottingham, University Park, Nottingham NG7 2RD, United Kingdom

[2]Department of Materials, Imperial College London, SW7 2AZ, London, United Kingdom

[3]School of Pharmacy, University of Nottingham, University Park, Nottingham NG7 2RD, United Kingdom

ABSTRACT: We investigated the feasibility of using spatially-offset Raman spectroscopy (SORS) for non-destructive characterisation of bone tissue engineering scaffolds. The deep regions of these scaffolds, or scaffolds implanted subcutaneously in live animals, are typically difficult to measure by confocal Raman spectroscopy techniques because of the limited depth penetration of light caused by the high level of light scattering. Layered samples consisting of bioactive glass foams (IEIC16), 3D-printed biodegradable poly-(lactic-co-glycolic acid) scaffolds (PLGA) and hydroxyapatite powder (HA) were used to mimic non-destructive detection of bio-mineralisation for intact real-size 3D tissue engineering constructs. SORS spectra were measured with a new SORS instrument using a digital micro-mirror device (DMD) to allow software selection of the spatial offsets. The results show that HA can be reliably detected at depths of 0-2.3 mm, which corresponds to the maximum accessible spatial offset of the current instrument. The intensity ratio of Raman bands associated to the scaffolds and HA with the spatial offset depended on the depth at which HA was located. Furthermore, we show the feasibility for *in-vivo* monitoring mineralisation of scaffold implanted subcutaneously by demonstrating the ability to measure transcutaneously Raman signals of the scaffolds and HA (fresh chicken skin used as a top layer). The ability to measure spectral depth profiles at high speed (5 s acquisition time), and the ease of implementation, make SORS a promising approach for non-invasive characterisation of cell/tissue development *in-vitro*, and for long-term *in-vivo* monitoring the mineralisation in 3D scaffolds subcutaneously implanted in small animals.

INTRODUCTION

Tissue engineering combines human cells and scaffold materials to grow tissues in the laboratory to replace diseased or damaged tissue parts in patients[1]. Tissue engineering is envisaged to fulfil the increasing demand for tissue grafts as well as to enable tailoring their biological properties to meet the requirements of individual patients (size, shape, immune-compatibility, etc). Vital to the further development of this technology and the associated widespread medical implementation of tissue engineering products is the availability of non-invasive techniques to monitor the *in-vitro* growth of the tissue. *In-vitro* studies are required to optimize the mechanical properties and biological activity of the scaffolds and engineered grafts. However, more relevant information regarding the clinical performance of the engineered tissues can be obtained from longitudinal *in-vivo* studies where the grafts are implanted in small animals. In such *in-vivo* studies, there is a need for non-invasive tools to monitor the temporal and spatial the development of the grafts after implantation, but at the same time minimize the number of animals used. For example, in bone tissue engineering, it is important to measure non-destructively the chemical properties of the tissue in order to monitor the formation and mineralization of the extracellular matrix throughout the entire graft. Currently, the performance of engineered tissue constructs is mostly assessed by conventional destructive methods, such as histological analysis[2].

Raman spectroscopy (RS) is a well-established analytical tool for measuring non-invasively live cells[3-6] and bone tissue[7-9]. RS has been used to measure the deposition of hydroxyapatite (HA) (the mineral phase of bone) on various types of bone tissue engineering scaffolds[10,11] and characterize the mineralization of osteoblast cultures *in-vitro*[12-15]. Because RS requires no exogenous labels, information regarding the composition of the mineral deposits and their evolution in time can be measured[1].

Nevertheless, the interrogation of cellular behavior and tissue/extra-cellular matrix formation at deeper depths within the 3D scaffold, by optical techniques still remains challenging.[17,18] So far, non-destructive RS measurements of scaffold-based tissue engineering constructs have been limited to monitoring the interaction of cell and biomaterial on the surface of 3D scaffold[10,19]. The porous scaffolds play a critical role in tissue engineering, as they provide a fine structure for cell seeding, proliferation and new tissue formation. However, the porous structure of the scaffolds (typical pore size 50-300 µm) leads to a high level of light scattering, thus limiting the penetration of light in the scaffolds. *In-vivo* measurements of grafts implanted in animals are even more difficult because of the need for light to penetrate through layers of soft tissue. Spatially-

offset Raman spectroscopy (SORS) is a novel technique for measuring depth-related chemical and physical properties of samples that exhibit high levels of light scattering, and has been verified as an effective tool for subsurface Raman analysis[20,21]. SORS allowed the measurement of subsurface chemical information in diffusely scattering samples, typically from depths of 20 μm – 5 mm range, which is beyond the reach of confocal RS. Furthermore, SORS has been used for *in-vivo* transcutaneous measurements of bone quality in small animals[22,23] and humans[24,25].

In this paper, we investigated the feasibility of using SORS for measuring non-destructively spectral depth-profiling of intact 3D bone tissue engineering scaffolds, under conditions mimicking both *in-vitro* growth and *in-vivo* development after subcutaneous implantation in patients or model animals. We present measurements on two common types of scaffolds: i) bioactive glass foams (IEIC16), scaffolds with a broad range of inter-connected pores (pore range 50-200 μm); ii) 3D-printed poly-(lactic-co-glycolic acid) scaffolds (PLGA), which had a well-defined structure with ~200 μm pores. Bioactive glass and PLGA are among the most popular and widely used materials for scaffolds in bone tissue engineering[26]. The former is a representative of bioactive materials able to bond to human tissue, while the latter represents the synthetic polymer family which exhibit tailorable and reproducible physical, chemical and biodegradation properties. Here, a SORS instrument based on a digital-mirror-device (DMD)[27] was used to measure Raman spectral depth-profiles of the scaffold/HA layered samples, demonstrating the potential of SORS to monitor the sub-surface mineralization of the scaffolds *in-situ*. The detection of HA is important in bone tissue engineering because the formation of hydroxyapatite (HA) within the scaffold is a step occurring to bone bonding, thus it is an indication of the scaffold bioactivity[26].

MATERIALS AND METHODS

Spatially offset Raman spectroscopy (SORS). All Raman spectroscopy measurements were carried out with a purpose-built SORS instrument based on a digital-mirror-device (DMD) to allow software selection of the spatial offsets. For excitation, the beam of a Ti:sapphire laser (3900S SpectraPhysics) tuned at 785 nm wavelength and 2 mm beam diameter, was focused on the sample by a 2×/0.06 NA microscope objective with 11 mm diameter entrance pupil (Olympus, Plan N). The laser power at the sample was 170 mW, and the diameter of the laser spot was illuminating an area of 88 μm. The back-scattered Raman photons were collected by the same objective, and focused by a lens (focal length 200 mm) onto a DMD (Texas Instruments, 0.30 WVGA chipset) connected to a PC using mini HDMI connection, and controlled by a home-built LabVIEW program. The DMD consisted of a 608 × 684 array of individually addressable micro-mirrors (7.6×7.6 μm²). The individual micro-mirrors can be switched to one of two states, 'on' and 'off', corresponding to a tilt of ±12°, allowing light at arbitrary spatial positions to be reflected towards the spectrometer (tilt +12°), whilst the remaining light is rejected (tilt -12°). The DMD was placed in the collection path of the Raman spectrometer at a sample-conjugate plane, serving as the offset controller for SORS, as well as a slit/pinhole for the spectrometer[27]. For all SORS measurements, a semi-annulus collection geometry was

selected, where the width of the annulus was 0.08 mm and the radius was defined by the spatial offset value (see Supporting Information Fig. S1). The area of the Raman collection region at the sample surface represented ~25% of the total area of the full annulus corresponding to a spatial offset value[27].

The Raman photons reflected by the DMD were collected by another lens (focal length of 100 mm), passed through a long filter (BLP01-785R-25, Semrock) and analyzed with an imaging spectrometer (Acton LS785, Princeton Instruments USA) with a 1000 g/mm plane ruled diffraction grating (Richardson Gratings, USA), and a 256×1024 pixel CCD camera (Newton BR-DD, Andor UK).

Tissue engineering scaffolds. Micrographs and scanning electron microscopy (SEM) images of the tissue engineering scaffolds investigated in this study are presented in Figure 1.

The composition of the IEIC16 bioactive scaffolds was 49.46 SiO_2, 36.27 CaO, 6.6 Na_2O, 1.07 P_2O_5 and 6.6 K_2O, in mol %. The scaffolds were produced by the gel cast foaming processing, as described elsewhere, where bioactive glass particle slurry is foamed with a surfactant and the foam set in place using a gelling agent (polymer) before sintering[28]. The modal interconnected pore diameter was 400 μm and interconnects estimated to be 100 μm measured by mercury porosimetry. The SEM image (Figure 1(b)) shows the interconnected macro-porous network, which can serve as template for tissue growth in 3D.

The poly-(lactic-co-glycolic acid) (PLGA) scaffolds (Figure 1(c) and (d) for the optical and SEM images) were 3D printed on a REGENHU 3D bioprinter. PLGA 85:15 (Mw= 50 kDa Evonik Industries) was extruded at a temperature of 120 °C onto a 50 °C heated platform. The printhead travelled at a speed of 12 mm/s and the pressure for printing PLGA was 4 bar.[29] The PLGA 3D-printed scaffolds have well-defined structure and regular pore size, and the distribution of pore size is centralized, result in a higher transparency and porosity, see Figure 1(c). SEM image (Figure 1(d)) reveals that the pore size is about 200 μm.

Hydroxyapatite powder ($[Ca5(OH)(PO4)3]x$), with particle size < 200μm, was purchased from Sigma Aldrich (CAS number: 12167-74-7). Fresh chicken skin samples (thickness 0.5 - 1 mm) were obtained from a local supermarket. Samples were kept at 4°C prior to measurements.

RESULTS AND DISCUSSION

SORS measurements of IEIC16 bioactive glass scaffold/HA/scaffold sandwiched structure. To mimic a measurement configuration for sub-surface detection of HA within an intact 3D porous scaffold, ~3 mm thick layer of hydroxyapatite (HA) powder was placed between two layers of IEIC16 foam, as schematically presented in Figure 2(a). The size of the sandwiched samples was 9 mm × 9 mm. The thickness of the scaffold sublayer was 1 mm, while the thickness of the top scaffold layer was varied (d = 0.5 mm, 1 mm and 2.0 mm) to mimic *in-situ* detection of HA at different depths within the 3D scaffold. Semi-annulus collection geometry was employed for all SORS measurements as it provides the high collection efficiency for the Raman photons.[27] The SORS spectra measured for the IEIC16 scaffold/HA layered samples are presented in Figure 2 (b) and (c), and compared to the Raman spectra of pure IEIC16 scaffold and HA powder. Figure 2 shows that the most intense band in the Raman spectrum of HA corresponds to the PO_4^{3-}

symmetric stretching at 962 cm^{-1}. The small peak at 1045 cm^{-1} also belongs to PO$_4^{3-}$ tetrahedral and corresponds to P-O asymmetric stretching. The Raman spectra of IEIC16 foams are dominated by a broad photoluminescence bands in the range 1200 - 2000 cm^{-1}. The SORS results in Figure 2(b) show that, for a IEIC16 top layer of 0.5 mm thickness, increasing the spatial offset value leads to an increase in the intensity of the Raman band associated to the HA sublayer (962 cm^{-1}) relative to 1390 cm^{-1} band assigned to the IEIC16 scaffold. Similar behavior is observed when the thickness of the top layer is increased to 1 mm and 2 mm. The results demonstrate that the sampling depth for SORS experiments of IEIC16 scaffold can be as deep as 2.0 mm, indicating the capability of SORS for depth profiling in scaffold-based tissue engineering study. Larger penetration depth may be achieved by replacing the DMD in the setup with one that has a larger active area, and/or by using a tube-lens with a shorter focal length when imaging onto the DMD, both of which will increase the available field of view for spatially-offset modulation.

Figure 3 shows the dependence of the relative intensities of the bands corresponding to the IEIC16 scaffold and HA on the spatial offset and the thickness of the scaffold top layer. The data were obtained by integrating the area under the Raman bands at 962 cm^{-1} and 1390 cm^{-1}. For both bands, local linear baselines were used for background subtraction. Three sets of data points were calculated from measured SORS spectra sample structures with IEIC16 scaffold top layer of thicknesses 0.5 mm, 1.0 mm and 2.0 mm. The results show that the Raman intensity ratio $R=I_{962}/I_{1390}$ increased as the spatial offset was increased, for all top layer thicknesses. When the thickness of the top layer was 0.5 mm, the ratio of Raman signals from the subsurface HA layer to surface IEIC16 layer, when changing the spatial offset from 0 to 1 mm, was R(1 mm)/R(0 mm)=~3.7. This value reduced to R(1 mm)/R(0 mm)=2 when the thickness of the top layer was increase to 2 mm. In addition, the absolute values of the I_{962}/I_{1390} ratio decreased as the thickness d of top scaffold layer increases. These findings are consistent with the increase in the number of detected Raman photons generated in the sub-surface HA layer when the spatial offset is increased: more photons generated in the deeper HA layer that are scattered towards the surface of the sample, and reach the surface at larger offset distance where they can be detected. However, increasing the spatial offset leads to a decrease in the number of detected photons generated in the top layers, as these photons typically reach the surface of the sample at lower offset values. Indeed, for a given spatial offset, increasing the thickness of the top layer leads to a higher contribution of Raman photons from the top layer and lower from the deeper layers.

Our results represent an important step forward from the earlier work. For example, Jones et al used Raman spectroscopy to monitor chondrocyte behavior on the surface of bioactive glass scaffolds[10] and Moimas et al investigated the effect of bioactive glass scaffold degradation in simulated body fluid over time[19]. However, these studies measured chemical and biological information non-destructively only from the surface of the scaffolds. Our results shown here demonstrate the feasibility of using SORS to sample deeper and retrieve information, such as mineralization, from sub-surface regions of bioactive scaffolds as deep as 2 mm.

SORS measurements on PLGA scaffold/HA layered structure.

SORS measurements on PLGA scaffolds with thickness of 0.8 mm, 1.7 mm and 2.3 mm were performed using the same DMD-based SORS instrument. A ~ 3 mm thick layer of HA powder at the back of the scaffolds to serve as a sublayer in the sample structure, see Figure 4(a). A thin quartz coverslip (0.17 mm thick) was placed in between the HA and the PLGA scaffold to prevent HA powder from penetrating into the pores of the scaffold. All the SORS results were obtained by the semi-annulus collection geometry using the DMD. To prevent direct illumination of HA in the sublayer through a pore, the laser beam was focused on a crossbar of the solid PLGA structure.

The SORS spectra are presented in Figure 4(b) and (c), respectively, and compared to the pure spectra of PLGA and HA. Spatial offset is indicated next to each Raman spectrum. For all spectra, a baseline was subtracted using a modified polynomial curve-fitting method described by Lieber et al [30]. The SORS spectra show that as the value of the spatial offset increased, the Raman band at 872 cm^{-1}, assigned to PLGA C-COO stretch vibration[31] gradually decreased relative to the Raman band at 962cm^{-1} assigned to HA increased. For thicker PLGA layers (Figure 4(c)) a similar trend was observed, although at zero spatial offset, no bands corresponding to HA can be detected in the Raman spectrum of the PLGA/HA scaffold. As the spatial offset is increased to 0.20 mm, the band at 962 cm^{-1} assigned to HA begins to emerge, and becomes dominant as the spatial offset is increased.

Figure 5 presents the Raman intensity ratio I_{962}/I_{872} as function of the spatial offset and the thickness of PLGA scaffold. The results show that, for all samples with different thickness of top layer, the Raman intensity ratio of I_{962}/I_{872} increased as the spatial offset was increased. For a thin top PLGA layer (0.8 mm), the $R=I_{962}/I_{872}$ increases rapidly when spatial offsets are larger than ~0.4 mm. The ratio of Raman signals from the subsurface HA layer to surface PLGA layer, when changing the spatial offset from 0 to 1 mm, was R(1 mm)/R(0 mm)=~2.8. A similar trend is observed when the thickness of the scaffold increases, but the ratio tended to plateau for larger spatial offsets (> 0.6 mm). For a 2 mm thick top-layer, the ratio R(1 mm)/R(0 mm)=~3. This observation may be used to link the rate of change of the measured ratio I_{962}/I_{872} as a function of the spatial offset to estimate the depth at which HA, i.e. mineralization, is found in an intact 3D scaffold.

Feasibility of detection mineralization for subcutaneously implanted scaffolds. After in-vitro optimization of the scaffolds, studies using animal models are typically used for assessing the performance of the tissue engineering scaffolds in more clinically relevant conditions. Subcutaneous implantation of engineered grafts in small animals is a common method to investigate different properties of the grafts, such as biocompatibility and bioactivity[32]. Suitable scaffolds should support and direct cell growth and tissue formation, replicate native 3D architecture, withstand mechanical and physiological loading and stresses, and exhibit function-dependent biodegradation without production of toxic by-products. Non-invasive tools for measuring the chemical profiles of the implanted grafts in-vivo are useful for measuring and monitoring these properties after implantation of the grafts.

After establishing the ability to measure spectral depth profiles of intact scaffolds and HA powder layers, we investigated whether HA could be detected in similar samples transcutaneously. To mimic such transcutaneous measurement conditions, layered samples based on fresh chicken skin, tissue engineering scaffolds (bioactive IEIC16 foam and 3D printed PLGA scaffold) and HA were prepared as schematically presented in Figure 6a. Figure 6b and c present the SORS spectra of these samples measured at different spatial offset values. Raman bands assigned to proteins and lipids can be identified at 1450 cm^{-1} (CH_2 deformations) and 1660 cm^{-1} (Amide I in proteins and C=C vibrations in and lipids)[3], allowing a relatively clear spectral window for the detection of the 962 cm^{-1} Raman band corresponding to HA. The results show that even at zero spatial offset, a weak peak at 962 cm^{-1} can be detected, in particular for the sample containing the PLGA scaffold. Bands corresponding to the PLGA (872 cm^{-1}) and IEIC16 bioactive glass are also detected. As the spatial offset is increased from 0 mm to 1 mm, the relative intensity of the 962 cm^{-1} band increases relative to the bands corresponding to the skin. These results demonstrate the feasibility to detect non-invasively scaffold mineralization at depths of several millimeters, in transcutaneous measurements. The fact that bands from both HA and scaffolds can be detected in the SORS spectra may be useful as their relative intensities could be used for estimation of the level of mineralization these scaffolds. At the same time, the intensity ratio of the bands corresponding to HA and skin may be used to estimate the depth at which the HA is located. While these results demonstrate the potential of SORS for *in-vivo* transcutaneous monitoring of bone tissue-engineering scaffolds, further work is required to optimize the optical design and develop models for extracting the relevant biological information from the SORS spectral depth-profiles.

CONCLUSION

Non-destructive spectral depth profiling of two common types of bone tissue engineering scaffolds, bioactive glass foams and biodegradable poly-(lactic-co-glycolic acid) (PLGA), was demonstrated by spatially offset Raman spectroscopy (SORS). The two types of scaffolds selected in this study had a random porous structure (bioactive IEIC16 foam) and regular structure obtained by 3D printing (PLGA scaffold). For the SORS experiments, an instrument based on a DMD was used in order to allow software selection of the spatial offset and rapid measurements of Raman spectra (typical signal-to-noise ratio >25 at 5 s integration time and 170 mW excitation power). In order to mimic *in-situ* detection of bone mineralization in the sub-surface regions of the scaffolds, layered samples of scaffold and hydroxyapatite (HA) powder were analyzed. The detection of HA in bone tissue engineering scaffolds is important because the formation of a hydroxyapatite layer on the surface of the scaffold is the step preceding to bone bonding. The results show that the detection of HA can be achieved through layers of 2.0 mm for IEIC16 foam and 2.3 mm for PLGA scaffold, values that correspond to the maximum spatial offset of the current instrument. The range may be extended by optimizing the optics at the DMD (active area and magnification). The results also show that the depth at which the HA is located in the scaffold can be estimated non-destructively by examining the intensity ratio of the measured Raman bands corresponding to the scaffold and HA. Furthermore, the ability to detect and measure HA in both bioactive glass and PLGA scaffolds through an intact layer of skin demonstrates the feasibility for *in-vivo* measuring the mineralization of tissue engineering grafts implanted subcutaneously in animal models. Although the laser power used here was higher than the safety standard relevant to laser light on the skin (BS EN 60825-1:2007) in order to allow short acquisition times (20 seconds), no damage was observed to the skin layer. This observation is consistent with previous reports of *in-vivo* confocal Raman micro-spectroscopy of skin[33], where a laser power of 100mW (730 nm wavelength) was focused to a spot of 1-2 μm (spot diameter in this study was 88 μm). Nevertheless, the feasibility of *in-vivo* transcutaneous SORS measurements using laser powers capped at the safety limits (10-30 mW) has been demonstrated previously, but at the expense of longer acquisition times (60 seconds)[25]. However, such longer acquisition times are acceptable for both *in-vitro* and *in-vivo* measurements of tissue engineering grafts, as the biological changes of interest, i.e. formation and mineralization of the extracellular matrix, occur over periods of days and weeks.

It is also important to mention the limitations of this study, mainly in terms of the phantom samples used. While two common types of scaffold were use, real tissue engineering grafts have a higher level of complexity. First, the presence of the collagen extracellular matrix may alter the light-scattering properties of the graft and generate additional Raman bands. The mineral composition of bone tissue is known to change during the development, including transformations in HA crystallinity. For *in-vivo* samples, further factors need to be considered, such as subcutaneous adipose tissue.

Nevertheless, these preliminary results demonstrate the feasibility of using SORS as tool for non-destructive characterization of scaffold-based tissue engineering constructs. This technique may be used for monitoring the development of the tissue *in-vitro* as well as for assessing its quality prior to clinical use. In addition, SORS may be used repeatedly to measure chemical spectral depth profiles, and may be a useful tool for long-term longitudinal studies on animal to monitor the temporal and spatial development of the tissue grafts. Apart from a potentially better understanding of the biomaterial properties, this technique may also allow a reduction in the number of animals used in such studies. However, further research is required to understand the photon migration within these samples and the origin of the SORS signals. Recent studies using bone layered samples investigated the relationships between the spatial offsets and the location of the probed volume within bone samples. [34,35] Similar systematic studies would allow the optimization of the SORS measurements conditions for tissue engineering grafts (sampling volume, range of spatial offsets), as well as develop models for recovering the relevant information out of the measured spectral depth profiles.

AUTHOR INFORMATION

Corresponding Author

* E-mail: ioan.notingher@nottingham.ac.uk

ACKNOWLEDGMENT

REFERENCES

(1) Langer, R.; Vacanti, J., Science **1993**, 260, 920-926.

(2) Doroski, D. M.; Brink, K. S.; Temenoff, J. S., Biomaterials **2007**, 28, 187-202.

(3) Notingher, I.; Hench, L. L., Expert Rev. Med. Devices **2006**, 3, 215-234.

(4) Kann, B.; Offerhaus, H. L.; Windbergs, M.; Otto, C., Adv. Drug Deliv. Rev. **2015**, 89, 71-90.

(5) Pascut, F. C.; Kalra, S.; George, V.; Welch, N.; Denning, C.; Notingher, I., Biochim. Biophys. Acta, Gen. Subj. **2013**, 1830, 3517-3524.

(6) Naemat, A.; Elsheikha, H. M.; Al-Sandaqchi, A.; Kong, K.; Ghita, A.; Notingher, I., Analyst **2015**, 140, 756-764.

(7) Rehman, I.; Smith, R.; Hench, L. L.; Bonfield, W., J. Biomed. Mater. Res. **1995**, 29, 1287-1294.

(8) Morris, M. D.; Finney, W. F.; Rajachar, R. M.; Kohn, D. H., Farad. Discuss. **2004**, 126, 159-168.

(9) Morris, M. D.; Matousek, P.; Towrie, M.; Parker, A. W.; Goodship, A. E.; Draper, E. R. C., J. Biomed. Opt. **2005**, 10, 014014.

(10) Jones, J. R.; Vats, A.; Notingher, L.; Gough, J. E.; Tolley, N. S.; Polak, J. M.; Hench, L. L. In Key Engineering Materials, Vols. 284-286, **2005**; pp 623-626.

(11) Kunstar, A.; Leferink, A. M.; Okagbare, P. I.; Morris, M. D.; Roessler, B. J.; Otto, C.; Karperien, M.; van Blitterswijk, C. A.; Moroni, L.; van Apeldoorn, A. A., J. R. Soc. Interface **2013**, 10, 20130464.

(12) Tarnowski, C. P.; Ignelzi, M. A.; Morris, M. D., J Bone Miner Res. **2002**, 17, 1118-1126.

(13) Gough, J. E.; Notingher, I.; Hench, L. L., J Biomed Mater Res A **2004**, 68A, 640-650.

(14) Jell, G.; Notingher, I.; Tsigkou, O.; Notingher, P.; Polak, J. M.; Hench, L. L.; Stevens, M. M., J Biomed Mater Res A **2008**, 86A, 31-40.

(15) Pully, V. V.; Lenferink, A.; van Manen, H.-J.; Subramaniam, V.; van Blitterswijk, C. A.; Otto, C., Anal. Chem. **2010**, 82, 1844-1850.

(16) Ghita, A.; Pascut, F. C.; Sottile, V.; Notingher, I., Analyst **2014**, 139, 55-58.

(17) Mather, M. L.; Morgan, S. P.; Crowe, J. A., Regen. Med **2007**, 2, 145-160.

(18) Leferink, A. M.; van Blitterswijk, C. A.; Moroni, L., Tissue Eng Part B Rev. **2016**, 22, 265-283.

(19) Moimas, L.; De Rosa, G.; Sergo, V.; Schmid, C., J Appl Biomater Biomech **2006**, 4, 102-109.

(20) Matousek, P.; Clark, I. P.; Draper, E. R. C.; Morris, M. D.; Goodship, A. E.; Everall, N.; Towrie, M.; Finney, W. F.; Parker, A. W., Appl. Spectrosc. **2005**, 59, 393-400.

(21) Matousek, P., Chem. Soc. Rev. **2007**, 36, 1292-1304.

(22) Schulmerich, M. V.; Finney, W. F.; Fredricks, R. A.; Morris, M. D., Appl. Spectrosc. **2006**, 60, 109-114.

(23) Schulmerich, M. V.; Cole, J. H.; Kreider, J. M.; Esmonde-White, F.; Dooley, K. A.; Goldstein, S. A.; Morris, M. D., Appl. Spectrosc. **2009**, 63, 286-295.

(24) Matousek, P.; Draper, E. R. C.; Goodship, A. E.; Clark, I. P.; Ronayne, K. L.; Parker, A. W., Appl. Spectrosc. **2006**, 60, 758-763.

(25) Buckley, K.; Kerns, J. G.; Vinton, J.; Gikas, P. D.; Smith, C.; Parker, A. W.; Matousek, P.; Goodship, A. E., J. Raman Spectrosc. **2015**, 46, 610-618.

(26) Jones, J. R., Acta Biomater **2013**, 9, 4457-4486.

(27) Liao, Z.; Sinjab, F.; Gibson, G.; Padgett, M.; Notingher, I., Opt. Express **2016**, 24, 12701-12712.

(28) Wu, Z. Y.; Hill, R. G.; Yue, S.; Nightingale, D.; Lee, P. D.; Jones, J. R., Acta Biomater. **2011**, 7, 1807-1816.

(29) Ruiz-Cantu, L.; Gleadall, A.; Faris, C.; Segal, J.; Shakesheff, K.; Yang, J., Biofabrication **2016**, 8, 015016.

(30) Lieber, C. A.; Mahadevan-Jansen, A., Appl. Spectrosc. **2003**, 57, 1363-1367.

(31) Geze, A.; Boury, F.; Benoit, J.-P.; Chourpa, I.; Dubois, P., Analyst **1999**, 124, 37-42.

(32) Gothard, D.; Smith, E. L.; Kanczler, J. M.; Black, C. R.; Wells, J. A.; Roberts, C. A.; White, L. J.; Qutachi, O.; Peto, H.; Rashidi, H.; Rojo, L.; Stevens, M. M.; El Haj, A. J.; Rose, F. R. A. J.; Shakesheff, K. M.; Oreffo, R. O. C., PLoS ONE **2015**, 10, e0145080.

(33) Caspers, P. J.; Lucassen, G. W.; Carter, E. A.; Bruining, H. A.; Puppels, G., J. Invest. Dermatol. **2001**, 116, 434-442.

(34) Sowoidnich, K.; Churchwell, J.; Buckley, K.; Kerns, J. G.; Goodship, A. E.; Parker, A. W.; Matousek, P., Proc. SPIE **2015**, 9540, 954009.

(35) Sowoidnich, K.; Churchwell, J.; Buckley, K.; Goodship, A. E.; Parker, A. W.; Matousek, P., J. Raman Spectrosc. **2016**, 47, 240-247.
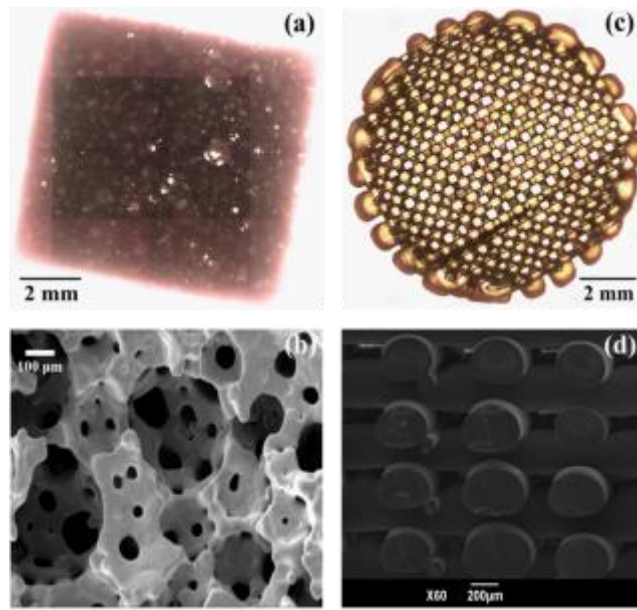
Figure 1. (a) Optical microscope image and (b) SEM image of an IEIC16 bioactive glass scaffolds. (c) Optical microscope image and (d) SEM cross-section image of a 3D printed PLGA scaffolds.
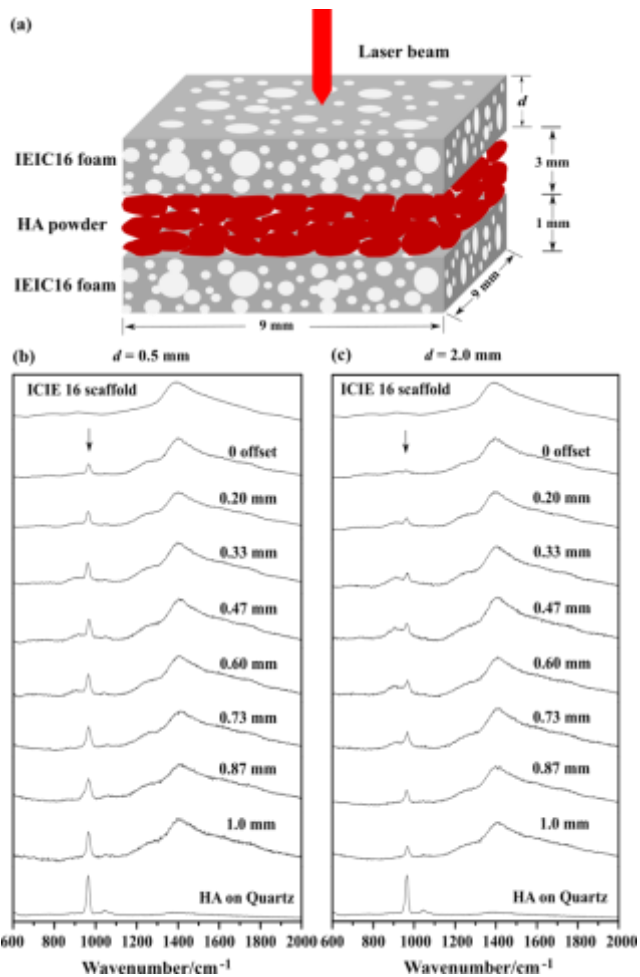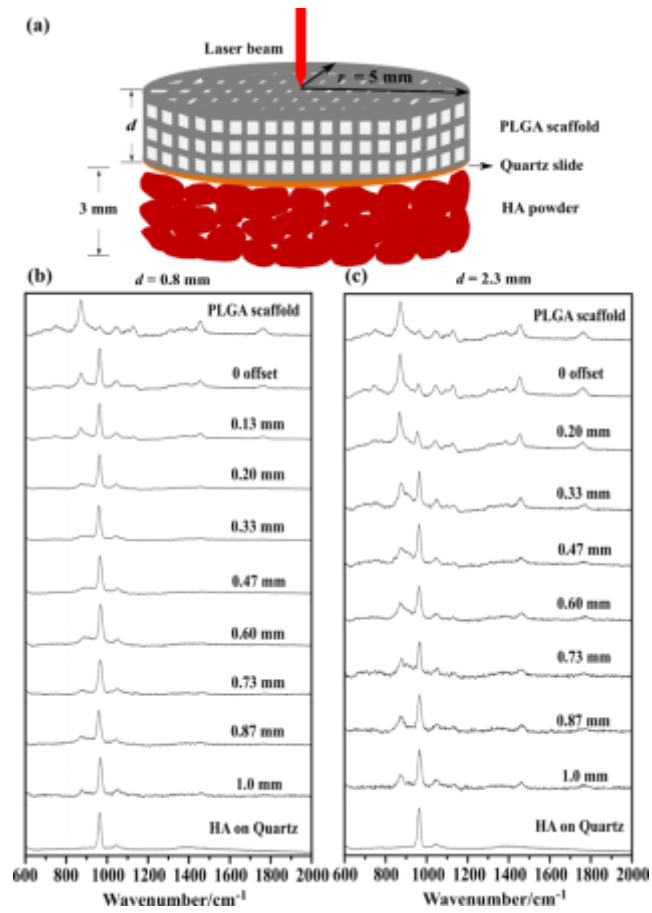
Figure 2. (a) Schematic description of IEIC16 scaffold/HA/scaffold sandwich structures used in the experiments for SORS measurement. A set of spatial offset Raman spectra obtained from the samples consisting of (b) top layer d = 0.5 mm and (c) top layer d = 2.0 mm IEIC16 scaffold and ~ 2 mm thick layer of HA powder. Spatial offsets are indicated next to each Raman spectrum. Integration time for each spectrum is 5 s. Raman spectra of IEIC16 scaffold and HA powder (measured separately) are also shown for comparison. All spectra were normalized with respect to the maximum intensity, and then shifted vertically for clarity.
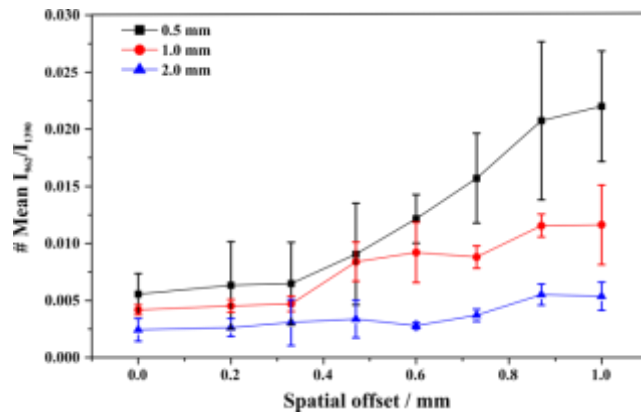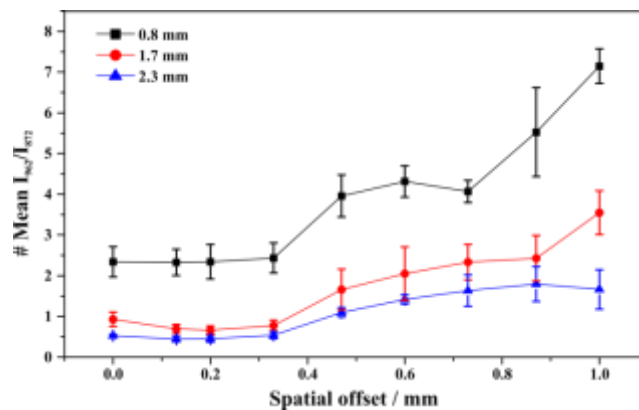
Figure 3. The ratio of Raman band intensity corresponding to the sub-surface HA layer (962 cm^{-1}) and top layer IEIC16 bioactive glass (1390 cm^{-1}) as a function of the spatial offset distance. The curves correspond to three thicknesses of the top layer: 0.5 mm, 1 mm and 2 mm. The mean values and standard deviations are obtained from three measurements on different locations on the sample.

Figure 4. (a) Schematic description of PLGA scaffold/HA layered structure. A quartz slide (~ 170 μm thickness) was placed in between the layers to prevent HA powder penetrate into the pores of the scaffold. A set of spatial offset Raman spectra obtained from the samples consisting of (b) top layer d = 0.8 mm and (c) top layer d = 2.3 mm PLGA scaffold, and ~ 3 mm thick of HA powder as lower layer. Spatial offset is indicated next to each Raman spectrum. Integration time for each spectrum is 5 s. Raman spectra of PLGA scaffold and HA powder (measured separately) are also shown for comparison. All spectra were normalized with respect to the maximum intensity, and then shifted vertically for clarity.

Figure 5. The ratio of Raman band intensity corresponding to the deep HA layer (962 cm^{-1}) and top PLGA layer (872 cm^{-1}) as a function of spatial offset distance. The curves correspond to three thicknesses of the top layer: 0.5 mm, 1 mm and 2 mm. The mean values and standard deviations are obtained from three measurements on different sample locations.
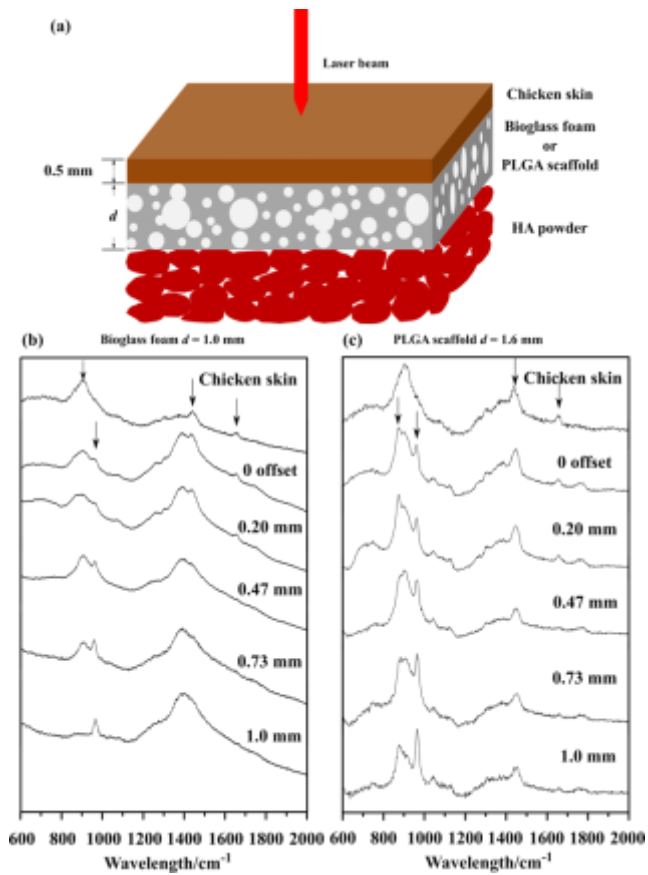
Figure 6. (a) Schematic description of IEIC16 bioglass and PLGA scaffold/HA layered structures used to mimic transcutaneous in-vivo SORS measurements (fresh chicken skin used as top layer). The size of the samples was ~10 mm x 10 mm x 6 mm. (b) SORS spectra measured at different spatial offset values. Integration time was 20 s for each spectrum. All spectra were normalized with respect to the maximum intensity, and then shifted vertically for clarity.

Insert Table of Contents artwork here